Input Current Harmonics Reduction in Non-isolated Buck-boost ZVS AC-DC LED Driver using Triangular Current Mode

Hiroki Watanabe[1]*, Daisuke Ueda[2], Jun-ichi Itoh[1]
1 Dept. of Electrical, Electronics, and Information Engineering, Nagaoka University of Technology, Nagaoka, Japan
2 Lighting Business Division, Panasonic Electric Works Co. Ltd, Osaka, Japan
*hwatanabe@vos.nagaokaut.ac.jp

***Abstract*—This paper proposes a low-order harmonics compensation method of the buck-boost PFC converter with triangular current mode (TCM) for LED driver applications. The TCM buck-boost PFC converter has the capability for power factor correction and wide output voltage regulation. Moreover, TCM reduces switching losses by enabling zero-voltage switching (ZVS). TCM is implemented using variable-frequency control to shape a triangular current with a negative current path. However, the nonlinear characteristics decay the power factor correction (PFC) performance. As a result, AC input current harmonics increase. The proposed control improves the quality of the AC input current in the TCM buck-boost PFC converter. The experiment confirms the validity of the proposed method. As the experimental result, it was confirmed that the 3rd-order harmonics in the AC input current are reduced by 70.3% at a grid voltage of 200 V_{rms} by the proposed method. Finally, maximum efficiency of the TCM buck-boost PFC converter reached 96.6%.**

Keywords—Buck-boost PFC converter, Triangular current mode, PFC, Zero-voltage switching.

I. Introduction

The light-emitting diode (LED) market has been growing due to its attractive advantages, including long lifetimes, low power consumption, and high luminance. It is well known that LEDs are driven by DC power. Therefore, the isolated or non-isolated AC-DC converter is commonly used to obtain DC power from a single-phase AC grid [1]-[6]. A two-stage converter with a diode bridge and a DC-DC converter is a simple configuration for LED drivers. Moreover, the PFC converter is often required to reduce harmonics in the AC input current.

The non-isolated DC-DC converter is divided into three types: boost, buck, and buck-boost converters. The boost converter is the most popular configuration. However, the minimum DC voltage is limited to the peak grid voltage. The buck converter realizes a low DC voltage. On the other hand, it is difficult to minimize input current harmonics when the buck converter operates as the buck-type PFC converter. Therefore, both a boost PFC converter and a buck DC-DC converter are adopted for low DC voltage situations.

The buck-boost PFC converter achieves wide DC voltage regulation. The buck-boost PFC converter operates under discontinuous current mode (DCM) or boundary current mode (BCM). Both current modes have low turn-on switching loss and no reverse-recovery loss. Moreover, BCM reduces conduction loss compared to DCM because its peak inductor current is lower. On the other hand, switching loss remains a problem when operating at higher switching frequencies.

The soft-switched buck-boost PFC converters have been widely considered [7]-[9]. Ref. [7] proposed a zero-voltage switching (ZVS) four-switch buck-boost converter. In this method, the inductor current is controlled as a trapezoidal waveform, with negative current flow, to reduce the current RMS. The negative current flow is used for ZVS operation because it discharges the parasitic capacitor of the switching device before turn-on. On the other hand, this converter requires four switch configurations, which increases costs.

Ref. [8] proposed a soft-switching buck-boost PFC converter with a common-ground configuration. This converter achieves ZVS and zero current switching (ZCS) using the resonance of the parasitic capacitor of switching devices and an additional coupled inductor. Moreover, the common-ground configuration is expected to eliminate common-mode noise due to a zero common-mode voltage. However, weight density may increase due to the addition of magnetic components, such as coupled inductors.

Ref. [9] proposed a soft-switching bridgeless buck-boost PFC converter. This converter consists of a bridgeless PFC converter and an auxiliary ZVS circuit. The auxiliary circuit is implemented for ZVS turn-on and ZCS turn-off operation of the PFC converter. This paper reported that the maximum efficiency reaches 97.3% under full-load conditions. On the other hand, this converter also requires a three-winding coupled inductor. Therefore, high weight is a concern.

The triangular current mode (TCM) is also a candidate for a soft-switching solution [10]-[12]. TCM achieves zero-voltage switching (ZVS) before the turn-on of the switching device by applying a slight negative current. The LED side of the buck-boost PFC converter uses a switching device instead of a diode to achieve negative inductor current flow and minimize conduction loss for TCM operation. Therefore, the buck-boost PFC converter with TCM is expected to achieve high efficiency in LED drivers. However, AC input current harmonics increase due to the variable switching frequency operation in TCM. Ref. [10] reports a two-switch buck-boost

PFC converter with TCM operation. This converter achieves ZVS operation by TCM. However, the input current harmonics increase.

This paper proposes a control method to reduce input current harmonics in a buck-boost converter operating in TCM mode. The contribution of this paper is that the low-order harmonics in the AC input current is compensated by simple feed-forward control for the TCM buck-boost converter without feedback control. Experimental results demonstrate the validity of the proposed control. Finally, the conversion efficiency is evaluated for both the BCM and TCM operations.

II. BUCK-BOOST PFC CONVERTER

Fig. 1 shows the circuit configuration of the buck-boost PFC converter. The synchronous rectifier reduces conduction losses in the AC-DC conversion stage. The switching timing of the synchronous rectifier follows the grid voltage (50 or 60 Hz) without Pulse Width Modulation (PWM). The buck-boost PFC converter achieves PFC capability and output current control for driving LEDs. The shunt resistor is added to the inductor current path to detect the zero-current timing of I_L for TCM. In the buck-boost PFC converter, a GaN-HEMT is used as the switching device for S1 and S2 to achieve high switching frequency operation, thereby reducing the size of inductor L_1. TCM aims to reduce switching losses in the buck-boost PFC converter. Moreover, it offers the attractive advantage of good DC current regulation for LED lighting control, owing to the high-speed command response of the inductor current I_L due to non-feedback current control.

Fig.2 shows the inductor current waveform and switching pattern of the buck-boost PFC converter. The inductor current I_L becomes the triangular current with a slight negative current. The secondary-side switching state for S2 is regulated by the zero-current signal from the shunt detector to define the negative current period T_d. Both S_1 and S_2 achieve ZVS owing to negative current flow, which discharges the parasitic capacitor on each switching device during the dead time before turn-on.

Fig.3 shows the operation mode of the buck-boost PFC converter. The details of each mode are as follows.

Mode 1: S1 still turns on, and the inductor current linearly increases until the end of mode 1. The peak current I_{peak} is expressed as

$$I_{peak} = \frac{|v_{ac}|}{L} T_{on} \tag{1}$$

where v_{ac} is the grid voltage, L is the inductance, and T_{on} is the on-time of S_1.

Mode 2 (dead time): The inductor current conducts to the secondary side of the buck-boost PFC converter through the free-wheeling diode of S_2.

Mode 3: S_2 turns on in this mode. The inductor current linearly decreases to zero. The relationship between inductor current and output voltage V_{LED} is expressed as

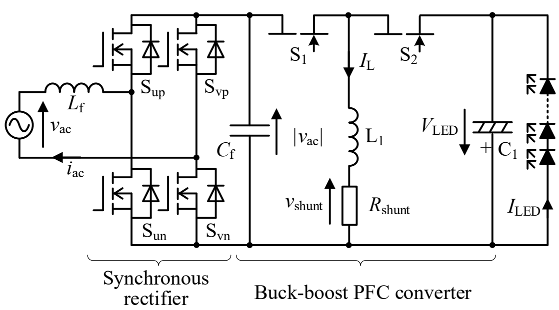

Fig. 1. Circuit configuration of non-isolated AC-DC converter with buck-boost PFC converter. Buck-boost converter operates based on triangular current mode to achieve ZVS.

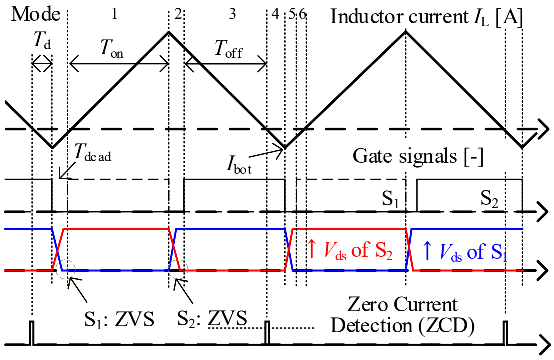

Fig. 2. Inductor current and switching waveforms of buck-boost PFC converter. TCM realizes zero voltage switching of S_1 by negative inductor current.

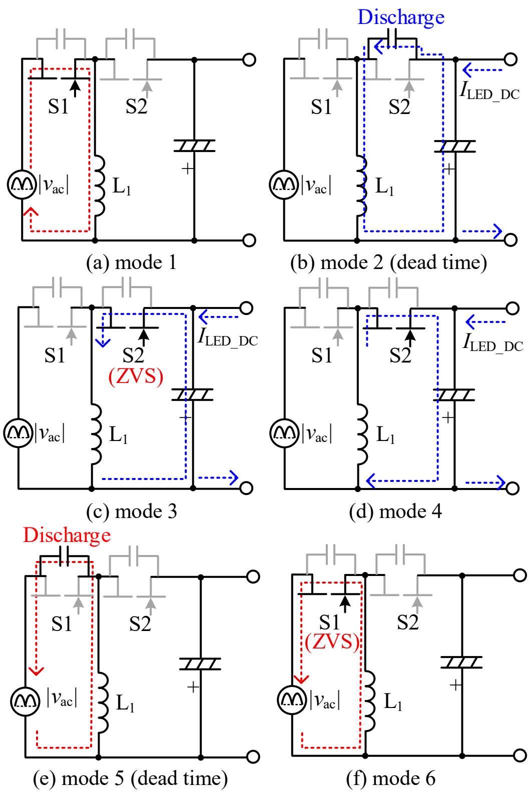

Fig. 3. Operation modes of buck-boost PFC converter. Both switch S_1 and S_2 achieves ZVS. Inductor current is controled as triangular waveform with small negative current for TCM.

$$I_{peak} = -\frac{V_{LED}}{L} T_{off} \tag{2}$$

where T_{off} is the on-time of S_2. In this mode, S_2 achieves

ZVS because the parasitic capacitor of S_2 is already discharged in mode 2.

Mode 4: The switching pattern is the same as mode 3. On the other hand, the inductor current path becomes negative from mode 3. This period determines the ZVS performance of the buck-boost PFC converter.

Mode 5 (dead time): S_2 turns off in this mode. The inductor current continuously flows through the primary-side current loop. In this period, the parasitic capacitor of S_1 is discharged by the inductor current. Finally, S_1 turns on by ZVS in mode 6.

III. TRIANGULAR CURRENT MODE

The current mode in the buck-boost PFC converter is classified as Continuous Current Mode (CCM), Discontinuous Current Mode (DCM), Boundary Current Mode (BCM), and TCM. DCM and BCM are preferred for the buck-boost PFC converter because of lower switching losses and no reverse-recovery losses compared to CCM. The DCM operation drastically reduces the input current harmonics by simple open-loop control. However, a large input current ripple requires a large Differential-Mode (DM) filter. On the other hand, the BCM operation reduces the peak current owing to the variable switching frequency, which eliminates the zero-current period. However, the switching loss due to the parasitic capacitor of the switching device becomes a drawback to improving efficiency.

TCM is implemented similarly to the BCM control strategy. The difference between BCM and TCM is that the negative inductor current in TCM contributes to achieving wide-range ZVS in each switching cycle because an additional switching state controls this current during the reverse-conductive period.

Fig.4 shows the switching frequency of BCM and TCM. In this mode, the switching frequency is adjusted based on the zero-current signal to maintain the boundary current condition. The switching frequency is BCM, and TCM is expressed as

$$f_{sw} = \frac{1}{\left(\frac{|v_{in}|}{V_{dc}}+1\right)T_{on}} \quad (3)$$

where f_{sw} is the switching frequency, T_{on} is the on-time of S_1. The inductor current I_L increases linearly during mode 1, which is determined by T_{on}. Therefore, T_{on} affects the output power condition. According to Fig. 4, the switching frequency of both BCM and TCM differs according to the grid voltage. Especially, the switching frequency reaches a maximum around the zero-crossing of the grid voltage. Comparing the switching frequency of each current mode, TCM decreases the switching frequency because the peak-peak current increases due to the negative current for ZVS. The negative current I_b is determined to discharge the parasitic capacitor of S_1. Therefore, it is calculated by the capacitor energy, and the inductor energy of L_1 for discharge of the capacitor [13].

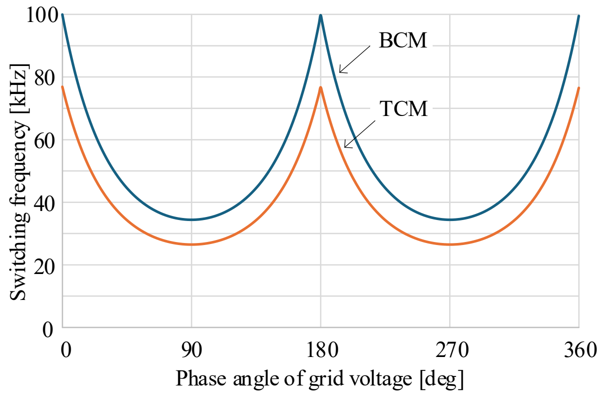

Fig. 4. Switching frequency of BCM and TCM when grid voltage is 100 V_{rms}.

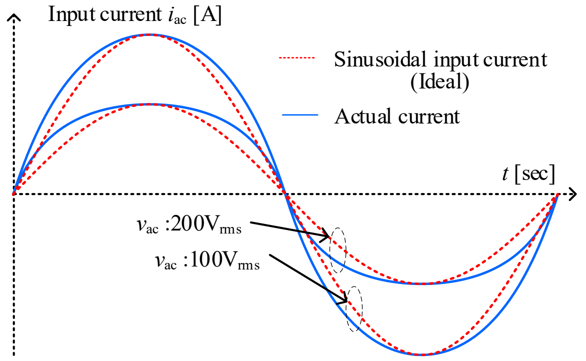

Fig. 5. Input current waveforms according to grid voltage v_{ac}. Input current harmonics increases due to non-linear characteristics by variable switching frequency under TCM operation.

IV. INPUT CURRENT HARMONICS REDUCTION

Fig. 5 shows the input current waveforms under TCM. The buck-boost PFC converter adjusts the inductor current I_L to a full-wave rectified waveform for power factor correction. The DCM buck-boost PFC rectifier achieves high-performance PFC because the ideal inductor average current is achieved in DCM. The inductor average current under DCM $I_{L\_ave\_DCM}$ is expressed as

$$i_{L\_ave\_DCM} = \frac{|v_{ac}|}{2L} D_{on}^{2} T_{sw} \quad (4)$$

where D_{on} is the on-duty S1, and T_{sw} is the switching cycle. Note that the average current is the average value of the ripple current, including the switching frequency component. According to (4), the average current waveform under DCM is the same as |vac| when the on-duty and switching cycles are set to constant. As a result, the input current i_{ac} becomes a non-distorted sinusoidal waveform.

On the other hand. The TCM buck-boost rectifier operates at a variable switching frequency. The inductor average current under TCM $i_{L\_ave\_TCM}$ is expressed as

$$i_{L\_ave\_TCM} = \left(\frac{V_{LED}}{|v_{ac}|+V_{LED}}\right)\frac{|v_{ac}|}{2L} T_{on} \quad (5)$$

where V_{LED} is the output DC voltage, T_{on} is the on-time of S_1.

In DCM, the relationship between the inductor average current and $|v_{ac}|$ becomes linear characteristics because the on duty and the switching cycle are the constant value. However, the inductor average current in TCM is nonlinear due to the variable switching frequency. As a result, input current harmonics increase as shown in Fig. 5. In this paper, the input current harmonics reduction method is proposed to improve the PFC performance of the TCM buck-boost PFC converter.

Fig. 6 shows the proposed control block diagram of the buck-boost PFC converter. The proposed control adjusts the on-time command T_{on}^* of S_1 to eliminate the nonlinear characteristics. In the proposed method, the on-time command is adjusted by the following, expressed as

$$k_{comp} = \frac{|v_{ac}| + V_{LED}}{V_{LED}} \tag{6}$$

where k_{comp} is the compensation coefficient for T_{on}^*. The gate signals of the synchronous rectifier are generated based on the detected grid voltage v_{ac}, and polarity detection. The switching frequency is set to 50 or 60 Hz, which corresponds to the grid frequency.

Fig. 7 shows the simulation results of input current waveforms when the grid voltage conditions of 100 V_{rms} and 200 V_{rms}. In this simulation, the input current distortion with and without the proposed control is evaluated under two conditions of the grid voltage: 100 V_{rms} and 200 V_{rms}. Note that the inductance L_1 is 4.5 mH, and the output power is 20 W. According to Fig. 7(a) and (b), the input current without the proposed control is distorted by the nonlinear characteristics, as shown in (6). On the other hand, the input current becomes a sinusoidal waveform when the proposed control is applied.

V. EXPERIMENTAL RESULT

A prototype circuit with rated power of 20 W is tested in order to confirm the validity of the proposed method. Table I shows the experimental parameters. In the experiment, two grid voltage condition of 100 V_{rms} and 200 V_{rms} are tested because of the wide input voltage condition. The switching frequency range of the TCM buck-boost PFC converter is changed corresponding to the grid voltage. Especially, the switching frequency increases when the grid voltage is 200 V_{rms} owing to low input current.

Fig. 8 shows the input and output waveforms when v_{ac} is 100 V_{rms}. In this condition, the TCM buck-boost converter is operated as the boost converter to obtain the output voltage of 200 V from input voltage of 100 V_{rms}. According to Fig. 8 (a) and (b), it was confirmed that the input current comes close to the sinusoidal waveform when the proposed control is applied. Note that the input current near the zero-crossing point is still distorted because of the switching frequency limitation. It will be improved by the rework of the zero-current detection of the buck-boost PFC converter.

Fig. 9 shows a comparison of input current harmonics to confirm the reduction of low-order harmonics by the proposed method. According to Fig. 9, the 3rd-order harmonics should be compensated to improve the input current quality because its harmonics are higher than the other harmonic components. As the analysis result, the proposed control reduced the third-order harmonics by 37.4% compared to without the proposed control.

Fig. 10 shows the input and output waveforms when v_{ac} is 200 V_{rms}. In this experiment, the TCM buck-boost converter is operated in buck-boost mode. According to Fig. 10(a) and (b), it was confirmed that the proposed control improves the input current quality by reducing low-order harmonics, as shown in Fig. 7. Compared with Fig. 8 and 10, the current

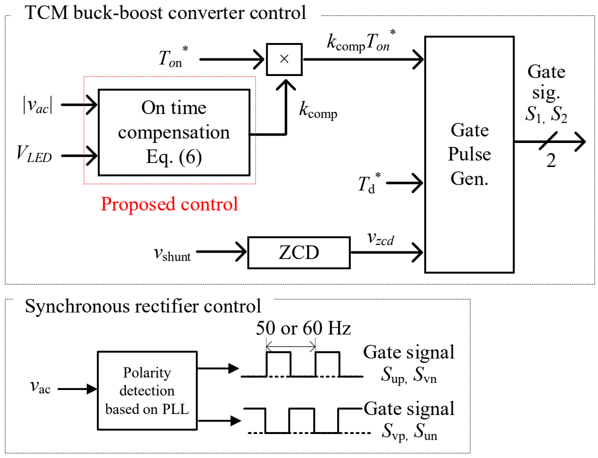

Fig. 6. Control block diagram of TCM buck-boost PFC converter.

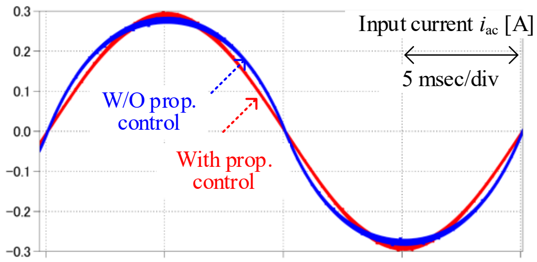

(a) Input current when V_{ac} is 100 V_{rms}

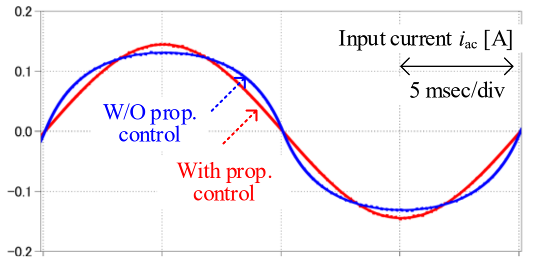

(b) Input current when V_{ac} is 200 V_{rms}

Fig. 7. Input current waveform comparison when proposed control is applied in simulation.

Table I Experimental parameters.

Symbol	Quantity	Value
V_{ac}	Grid voltage	100/200 V_{rms}
P_{rated}	Rated power	20 W
f_{sw}	Switching frequency	15-47 kHz (100V_{rms}) 31-100 kHz (200V_{rms})
V_{LED}	Output DC voltage	200 V
L_1	Inductance of PFC conv.	4.5 mH
L_f	Filter inductance	1 mH
C_f	Filter capacitance	1 µF
C_1	DC side capacitor	180 µF
R_{shunt}	Shunt resistor	1.68 Ω

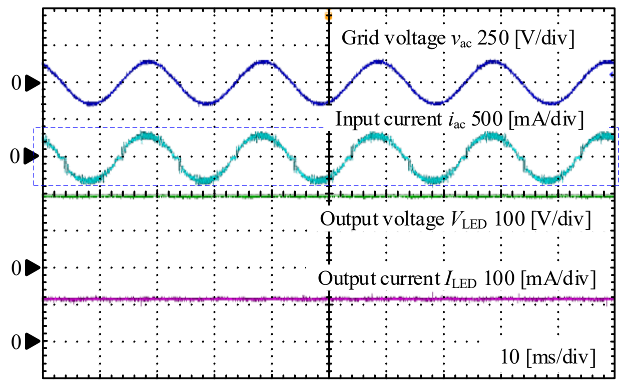

(a) Without proposed control

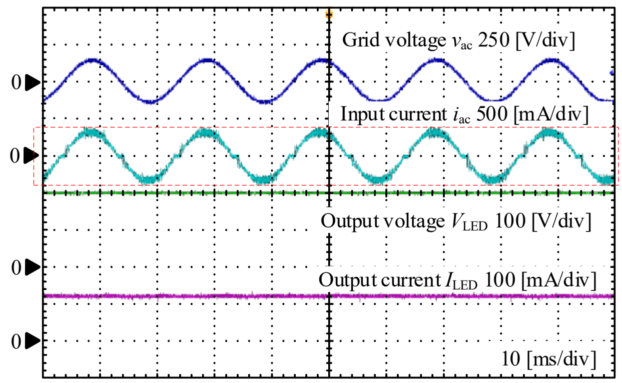

(b) With proposed control

Fig. 8. Experimental result when grid voltage is 100 V_{rms}.

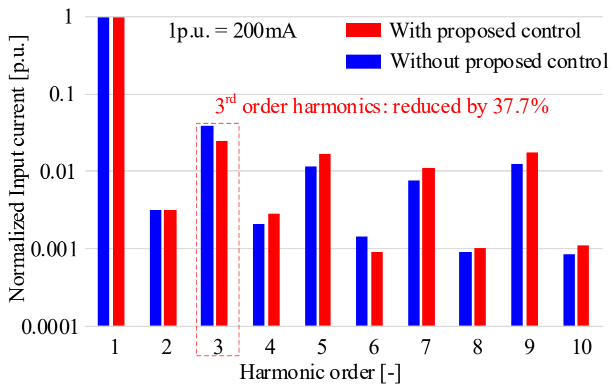

Fig. 9. Input current harmonics when grid voltage is 100 V_{rms}.

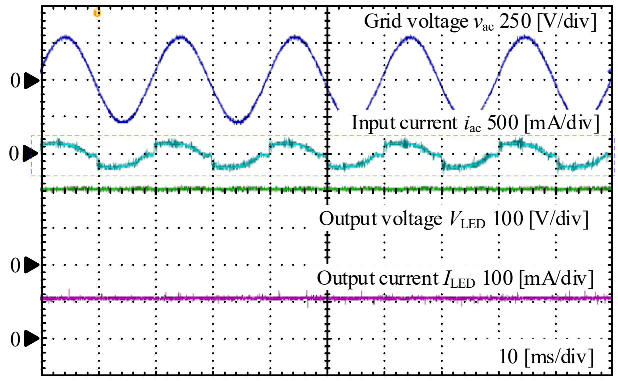

(a) Without proposed control

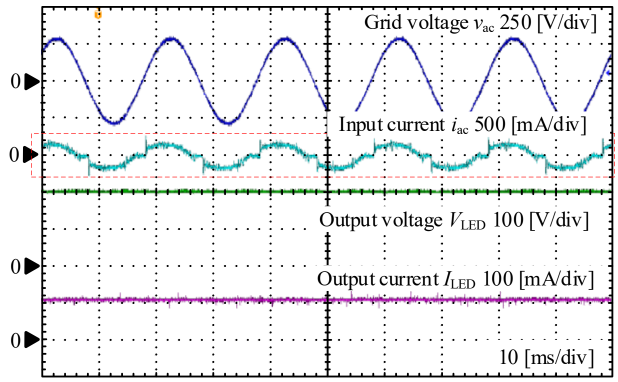

(b) With proposed control

Fig. 10. Experimental result when grid voltage is 200 V_{rms}.

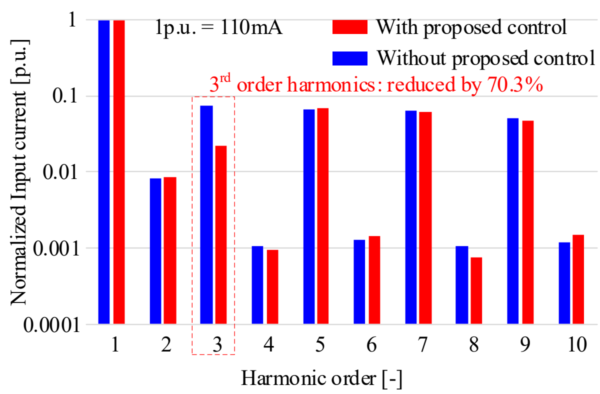

Fig. 11. Input current harmonics when grid voltage is 200 V_{rms}.

distortion increases when the grid voltage is 200 V_{rms}. This is because the fundamental component of 50 Hz is small due to the high grid voltage condition. As a result, the low-order harmonics affect the input current waveform more.

Fig. 11 shows the comparison of input current harmonics when the grid voltage is 200 V_{rms}. According to Fig. 11, odd-number harmonics of 3rd, 5th, and 7th become higher than Fig. 8. Comparing to the input current harmonics, it was confirmed that the proposed control reduces the 3rd order harmonics by 70.3%.

Fig. 12 shows the switching waveform of the buck-boost PFC converter. According to Fig. 12(a), hard switching occurs due to BCM operation. On the other hand, the drain-source voltage reaches zero before turn-on under TCM, as shown in Fig. 12(b). As a result, it was confirmed that ZVS is achieved by the negative inductor current owing to the proposed control. Moreover, the GaN-HEMT of S_2 achieves ZVS because the device current always flows from the source side, which means the parasitic capacitor is discharged before S2 turns on.

Fig. 13 shows the efficiency comparison of BCM and TCM. According to Fig. 12, TCM improved efficiency through ZVS. The peak efficiency of the TCM buck-boost PFC converter reached 96.6% at a grid voltage of 100 V_{rms}. Especially, the light-load efficiency is significantly improved when TCM is applied. This is because the switching frequency increases at low output power conditions. As a result, switching losses affect efficiency more at low power than at rated power. Compared to the efficiency curve between 100 V_{rms} and 200 V_{rms}, the efficiency is significantly improved at 200 Vrms owing to reduced switching losses.

VI. Conclusion

This paper proposed an AC input current-harmonics reduction technique for the TCM buck-boost PFC converter in LED driver applications. The proposed control improved the quality of the AC input current by adjusting the on-time command in the TCM. The experiment confirmed the validity of the proposed method. As the experimental result, it was confirmed that the 3rd-order harmonics in the AC input current is reduced by 70.3% by the proposed method when the grid voltage is 200 V_{rms}. Finally, maximum efficiency of the TCM buck-boost PFC converter reached 96.6%.

REFERENCES

[1] A. Escultero, C. M. Odulio,"Performance Analysis of Constant Current LCC Resonant LED Driver", *IEEE Energy Conversion Congr. Expo*, pp.3923-3929, 2024.

[2] J. M. Alonso, G. Z. Abdelmessih, M. A. Dalla Costa, Y. Guan, Y. Wang,"Investigation of the Use of Switched Capacitor Converters as LED Drivers", *IEEE Trans.Ind. Appl.*, Vol. 61, No. 1, pp.1305-1317. 2025.

[3] Y. Huang, D. B. Ma,"A Smart Silicon Carbide LED Driver IC With Integrated Dual-Level Condition-Monitoring Mechanism", *IEEE Tran. Power Electron.*,Vol. 39, No. 5, pp.6246-6255. 2024.

[4] P. Quintana-Barcia, S. Saeed, J. Ribas, J. Garcia, M. Perdigao,"Analysis of a dimmable quasi-resonant LED driver with variable inductor magnetic control", *IEEE Energy Conversion Congr. Expo.*, pp.7241-7248, 2024.

[5] Y. Wang, J. Xu, Z. Chen, F. Qin,"Small Signal Modeling and Transient Cross-Regulation Analysis of Peak-Current-Mode-Controlled SIDO Buck LED Driver", *IEEE Tran. Power Electron.*,Vol. 38, No. 10, pp.12834-12845, 2023.

[6] N. Molavi, H. Farzanehfard,"A Non-isolated Wide-Range Resonant Converter for LED Driver Applications", *IEEE Tran. Power Electron.*,Vol. 70, No. 9, pp.8939-8946, 2023.

[7] Y. Jiang, X. Ruan, F. Liu,"A Zero-Voltage-Switching Four-Switch Buck-Boost PFC Converter", *IEEE Jour.Emerging and Selected Topics in Power Electron.* (Early access), 2025.

[8] M. Maghsoudi, H. Farzanehfard,"Fully Soft-Switched Buck–Boost Bridgeless PFC Converters With Single-Magnetic Core" , *IEEE Tran. Power Electron.*,Vol. 71, No. 1, pp.419-426, 2024.

[9] M. Ghorbanian, M. Maghsoudi, F. Hosseinabadi, E. Adib, R. Barzegarkhoo, F. Blaabjerg,"A Soft-Switching Bridgeless Buck-Boost Power Factor Correction Converter With Simple Auxiliary Circuit and Low Input Current THD", *IEEE Jour.Emerging and Selected Topics in Power Electron.*,Vol. 11, No.4, pp.4245-4254, 2023.

[10] J.-W. Yang, H.-L. Do,"High-Efficiency ZVS AC-DC LED Driver Using a Self-Driven Synchronous Rectifier", *IEEE Trans. Circuits and Systems*, Vol.61, No. 2505-2512, 2014.

[11] D. Nguyen, Y. Liu, X. Chen, and H. Chiu, "GaN-Based Interleaved Four-level FlyingCapacitor Triangular Conduction Mode (TCM) Converter with Coupled Inductors", *IEEJ Jour. of Ind. Appl.*, Vol. 13, No. 6, pp. 645-654, 2024.

[12] H. Watanabe and J. Itoh, "Development of Current-Fed DAB Converter Applying Triangular Current Mode forWide Voltage Applications", *IEEJ Jour. of Ind. Appl.*, Vol. 12, No. 4, pp. 726-734, 2023.

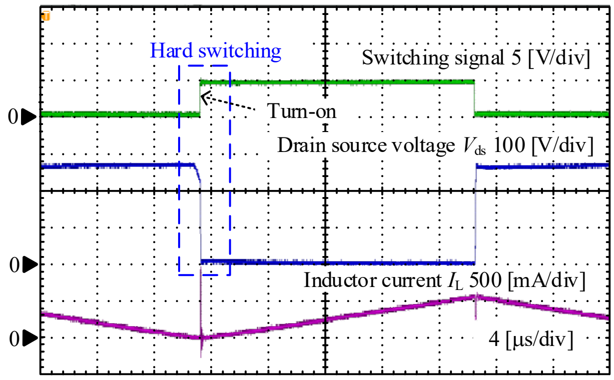

(a) Switching waveform under BCM.

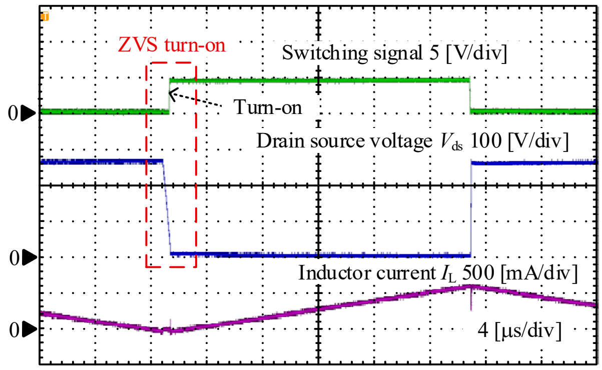

(b) Switching waveform under TCM.

Fig. 12. Switching waveforms of buck-boost PFC converter.

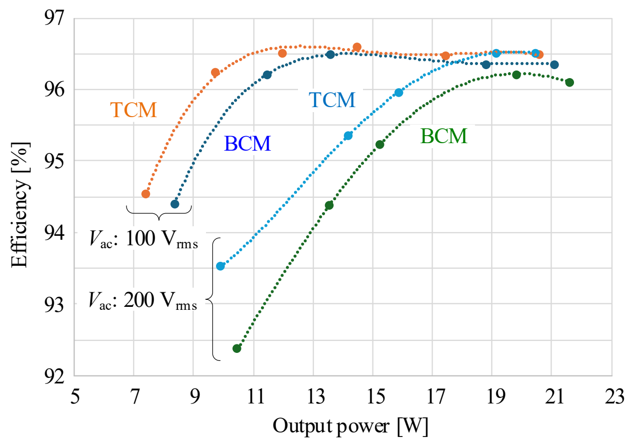

Fig. 13. Efficiency comparison of BCM and TCM.

[13] C. Marxgut, F. Krismer, D. Bortis, J. W. Kolar,"Ultraflat Interleaved Triangular Current Mode (TCM) Single-Phase PFC Rectifier", *IEEE Tran. Power Electron.*,Vol. 29, No. 2, pp.873-882, 2014.